Polymer Chemistry

PAPER

View Article Online
View Journal | View Issue

Cite this: *Polym. Chem.*, 2017, **8**, 2675

Facile synthesis of oligo(3-hexylthiophene)s conductive wires with charge-transfer functions†

Gözde Öktem,[a,b] Karin Sahre,[a] Brigitte Voit,[a,c] Rainer Jordan[b,c] and Anton Kiriy*[a,c]

Received 13th March 2017,
Accepted 31st March 2017

DOI: 10.1039/c7py00428a

rsc.li/polymers

A series of fully conjugated oligo(3-hexylthiophene)s bearing different starting- and end-groups have been synthesized by means of externally initiated Kumada catalyst-transfer polymerization (KCTP) and Grignard Metathesis Polymerization (GRIM). These kinds of oligomers' starting- and end-groups include *tert*-butyl protected thiols to be used for binding of oligomers to gold electrodes and tetracyanobutadiene-based donor–acceptor (DA) end-groups, such as dimethylaniline-tetracyanobutadiene (DMA-TCBD) and ferrocene-tetracyanobutadiene (Fc-TCBD), introduced to control the charge transport through the oligomers. The DMA-TCBD and Fc-TCBD end groups were incorporated by means of a Diederich-type click transformation of appropriately end-terminated oligo(3-hexylthiophene)s. The efficiency of the end-group functionalization was comprehensively assessed by NMR spectroscopy and MALDI-TOF spectrometry whereas the redox activities of the DA end-groups were examined by cyclic voltammetry. KCTP showed a much superior performance compared to GRIM in the introduction of a desirable end-group functionality. The thus-prepared conjugated oligomers are attractive materials for application in molecular electronics which will be explored in future studies.

Introduction

The bottom-up integration of tailor-made molecular structures designed as nanoscale building blocks to investigate electron transport properties is a rapidly emerging field.[1] The electron transport in a single molecule junction, where a single molecule bridges two metal electrodes, strongly depends on the degree of π-conjugation, the energy alignment, and the strength of a metal–molecule coupling.[2] Conjugated molecules containing alternating single and double bonds can delocalize electrons through their π-system, which is the first requirement for the molecule to function as a molecular wire. For efficient electron transport, a good overlap between the conduction orbital of the molecular wire and the Fermi level of the electrode should be achieved. Furthermore, the transport mechanism strongly depends on π-conjugation: it changes from a tunneling to a hopping in cases when π-conjugation is disrupted or when the π-system is too long.[3] Finally, metal-specific anchoring groups which serve as "molecular alligator clips" are needed for attachment of the molecular wire to metal electrodes.[4] Thiol-groups have been proven to be one of the most useful connectors of molecular wires to gold electrodes.[5] However, because "naked" thiol groups are too reactive to survive during the synthesis of molecular wires, they have to be protected. Acetyl, 2-(trimethylsilyl)ethyl, 2-cyanoethyl, 2-(4-pyridinyl)ethyl, methyl and *tert*-butyl (^{t}Bu) groups are widely used protecting groups for thiols.[6] Besides the thiol group, nitrogen-based functional groups, such as amino- or cyano-groups, have also been used for attachment of molecular wires to metal electrodes.[7] The presence of two different anchoring groups in the same molecule paves a way for fabrication of asymmetric molecular devices, such as diodes/rectifiers.

To date, various bottom-up methods have been developed to assemble molecular wires into molecular junctions including attachment of wires to electrodes,[8] stepwise growth of wires on electrode surfaces,[9] and interconnection of electrodes by *in situ* synthesis of wires.[10] So far, a dominating strategy for the preparation of molecular wires is a stepwise organic synthesis based mostly on metal-catalyzed cross-couplings such as Stille, Suzuki–Miyaura, Heck and Sonogashira reactions.[11,12] Although these methods allow the preparation of structurally well-defined molecules having a precisely controlled number of repeat units, the preparation procedures are complex as they involve numerous synthetic and purification steps.[11] Especially difficult is the synthesis of long molecular wires because of both the increasing number of synthetic steps and drastically

[a]*Leibniz-Institut für Polymerforschung Dresden e.V., Hohe Straße 6, 01069 Dresden, Germany. E-mail: kiriy@ipfdd.de*
[b]*Chair of Macromolecular Chemistry, Technische Universität Dresden, Mommsenstraße 4, 01069 Dresden, Germany*
[c]*Center for Advancing Electronics Dresden (CFAED), Technische Universität Dresden, 01062 Dresden, Germany*

†Electronic supplementary information (ESI) available: Detailed experimental procedures for KCTP and GRIM polymerizations, synthesis of model compounds and data for additional characterization by SEC, NMR, CV and UV-VIS. See DOI: 10.1039/c7py00428a

decreasing solubility of longer conjugated oligomers which greatly complicates the purification procedure. To overcome insolubility, conjugated oligomers can be modified with saturated alkyl side groups; however, care should be taken in designing of soluble oligomers because improperly introduced solubilizing groups may cause twist of the backbone due to steric hindrances between adjacent units which suppress electron transportation through the wire.[13]

In the present work we are interested in the structure of regioregular head-to-tail (HT) substituted oligo(3-hexylthiophene) (rr-O3HT) because their polymeric analogue, HT-poly (3-hexylthiophene) (rr-P3HT), represents one of the most successful examples of how an insoluble polymer (unsubstituted polythiophene) can be converted into a highly soluble one not only without degradation but rather with a clear improvement of the electronic properties.[14] A high degree of HT regioregularity in rr-P3HT has significant importance because the head-to-head linkage along the chain breaks the effective conjugation due to steric hindrances of the alkyl chains which forces thiophenes out of planarity.[15]

Syntheses of well-defined thiophene-based oligomers, as well as rr-O3HT, have been reported by several groups, however, the preparation procedures are tedious.[16] Recently, a Fibonacci-type synthesis of structurally well-defined regioregular HT oligo(3-hexylthiophene) molecules with a precisely controlled length up to 36 repeat units was also presented.[17] Although the Fibonacci's route shortens the number of synthetic steps comparably to other approaches, the overall yields of the final oligomers are relatively low. It should be stressed that the Fibonacci's route, as well as many syntheses of relatively long thiophene-based oligomers, provides only access to oligomers which have no end-groups suitable for binding to electrodes. On the other hand, incorporation of such groups in the very last synthetic step is especially difficult in the case of very long molecules. Therefore, the synthesis of relatively long rr-O3HT equipped with "molecular alligator clips" suitable for satisfying the needs of molecular electronics is still a challenge.

Alternatively, long π-conjugated chains can be constructed in a single chemistry step by means of polymer chemistry methods. However, most of the polymerization techniques involve a step-growth mechanism which assumes a random coupling of monomers. This approach does not allow sufficient control over the molecular length and the end-group functionality, which are crucial requirements for the material to be used in molecular electronics.[18] Among polymerization methodologies developed to date, Kumada catalyst transfer polycondensation (KCTP) is one of the most promising ways to synthesize well-defined end-functionalized oligomers and polymers.[19] Due to the intramolecular catalyst-transfer mechanism, polymer chains in KCTP grow in a one-by-one manner,[19–28] as each Ni catalyst species forms only one polymer chain. As such, a desirable degree of polymerization (DP) can be controlled by the monomer to initiator ratio, $[M_0]/[I]$.[19–28] In general, end-groups into P3HT chains can be incorporated either by transferring functions from the initiator (to form a *starting group via* externally-initiated KCTP firstly developed by Kiriy *et al.*[29–31] or by introducing an *end-group* in a chain-termination process *via* Grignard Metathesis polymerization (GRIM), as demonstrated in the early works of McCullough *et al.*[32] By using these approaches, one can prepare polymers having either only one end-functionality (*i.e.*, either starting or end groups), or functionalities from both sides (*i.e.*, starting and end groups).[33] Although in general, externally-initiated KCTP should be suitable for the preparation of bis-end-functionalized P3HT, to date it has been mostly applied to the synthesis of mono-functionalized P3HT, having carboxy-, hydroxy-, amino-,[34] phosphonato-,[35] pyridine- or thiolo-starting groups.[33,36] The synthesis of a polymer relevant for the construction of molecular electronic devices, P3HT bis-functionalized by thiol-groups, was also reported, and the applied method for quenching the polymerization mixture by elemental sulfur provided 72% functionalization degree on both chain ends.[33] However, examples of polythiophenes having *different* starting- and end-groups remain extremely scarce in the literature.[37] Furthermore, we are not aware of literature reports describing P3HTs having different starting- and end-groups, both of them being relatively complex *functional* groups, *i.e.*, not being "simple" H, Br, alkyl or aryl groups.

In general, by varying the kinds of starting and end groups, one can not only tune the selectivity and binding strength of molecular wires to electrodes but also adjust charge injection/collection processes. In such a way, KCTP has great synthetic potential to provide access to "simple" molecular electronic building blocks such as molecular wires but also to more sophisticated structures, such as molecular rectifiers. At the same time, other molecular devices, such as molecular switches, transistors, *etc*., would also be highly desirable for the fabrication of even more complex molecular-based circuits. Such building blocks bearing special electronic functions can be designed by incorporation of dedicated chemical functionalities, *e.g.*, redox- or photo-active moieties, into the structure of molecular wires.[38] The goal of the present work is to extend the versatility of the KCTP-based synthetic toolbox for the preparation of functionalized conductive wires. Particularly, we aimed at the development of a general approach for the synthesis of oligo(3-hexylthiophene)s bearing not only specific starting and end-groups for attachment to electrodes but also having additional charge-transfer moieties which might be used for tuning the charge transportation through the wire.

Recently, a new efficient synthetic method for facile construction of complex electron-deficient moieties based on high-yielding addition reactions of a strong acceptor tetracyanoethylene (TCNE) to electron-rich alkynes has been developed by the group of Diederich.[39,40] This reaction is based on the [2 + 2] cycloaddition of TCNE to alkynes substituted by aromatic amines (or other electron-donors such as ferrocene, or azulene), followed by a cyclo-reversion, to form donor-substituted 1,1,4,4-tetracyanobuta-1,3-diene (TCBD) chromophores (see, for example, Scheme 1, step D).[41–43] This transformation proceeds quickly under mild conditions

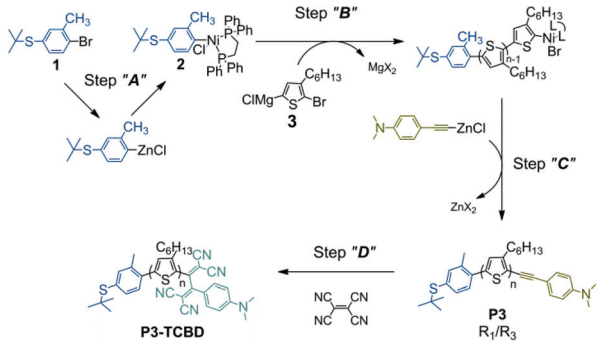

Scheme 1 Synthesis of oligomers exemplified by the preparation of **P3-TCBD**: step (A) synthesis of the initiator; step (B) KCTP; step (C) introduction of the end-group by Negishi coupling; and step (D) Diederich-type click reaction.

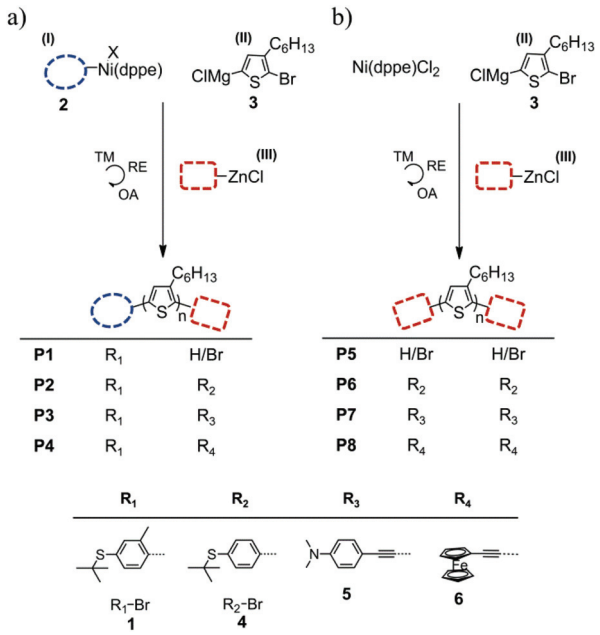

Scheme 2 Synthesis of oligomers with different starting/end groups by (a) externally-initiated KCTP and (b) Grignard metathesis polymerization. Reaction conditions: (I) **1**, *n*BuLi (–78 °C), $ZnCl_2$ (–78 °C), Ni(dppe)Cl_2 (RT); (II) 2-bromo-3-hexyl-5-iodothiophene, iPr-MgCl (0 °C); (III) **4**, **5** or **6**, *n*BuLi (–78 °C), $ZnCl_2$ (–78 °C).

without side reactions and byproducts and is therefore regarded as a click-type reaction.[39] This reaction has been used so far also for the incorporation of TCBD-based side-groups into polymers,[44] however, the synthesis of oligothiophenes having TCBD-based end-groups has not been reported so far.

Results and discussion

Scheme 1, steps A to C, shows the synthesis of double-end-functionalized rr-oligo3HTs which involves the combination of KCTP and Negishi cross-coupling. The first thiol functional group was introduced by transfer of a properly-substituted aryl group from a specially designed initiator to the starting group of the oligomer.

The initiator precursor contains a ^{t}Bu-protected thiol group (^{t}Bu-S) since it can tolerate a range of experimental conditions including strongly acidic and basic media. Furthermore, ^{t}Bu-S can be easily converted into a versatile thioacetate (AcS) moiety followed by its further conversion into completely deprotected thiol groups for immobilization onto desired gold electrodes.[45] The thiol group was placed into the *para*-position relative to the chain-propagating point because it was previously shown as an example of anthraquinone-based molecular wires that the *para*-substitution is the most favorable connection mode due to more efficient electron transport involving a quantum interference effect.[46] In addition, the methyl group at the *ortho*-position to the polymerization direction was introduced into the initiator precursor structure for stabilization of the Ni-initiator **2** (Scheme 1, step A).[31] On the other hand, the presence of the *ortho*-methyl group facilitates the preparation of the Ni-initiator from readily available Ni(dppe)Cl_2 and metal-organic precursors, as described in our previous work.[31]

To perform the externally initiated KCTP, initiator **2** was added to monomer **3** as in Scheme 2a at the monomer/initiator feed ratio of 10 : 1 and after the polymerization, the reaction mixture was divided into four parts to study the quenching process. The first portion was quenched with methanol (to introduce hydrogen as the end group) while the remaining three parts were quenched with the ZnCl-functionalized aryl compounds having either ^{t}Bu-protected aryl thiol (**4**), or ethynyl-*N*,*N*-dimethylaniline (ethynyl-DMA) (**5**), or ethynyl-ferrocene (ethynyl-Fc) (**6**). In another approach described in Scheme 2b, functionalized polymers were obtained *via* a classical GRIM method by adding monomer **3** to the Ni(dppe)Cl_2 catalyst in a monomer/initiator feed ratio of 10 : 1. Subsequently, the polymerization mixture was divided into three portions in order to be terminated with MeOH or different ZnCl-functionalized aryls **4**, **5** or **6**. After the quenching, the terminated products were extracted with chloroform and were further purified from low DP products *via* sequential Soxhlet extractions with acetone, hexane, and chloroform. The purified polymerization products were characterized in terms of starting-end group combinations, DPs, and dispersities.

It can be expected for a successful KCTP that all four polymerization products **P1**, **P2**, **P3** and **P4** will contain the same starting group (^{t}BuS(2-tol)), further designated as R_1 but different end groups: H (or Br) in **P1**, ^{t}BuS(Ph) (further designated as R_2) in **P2**, ethynyl-DMA (further designated as R_3) in **P3** and ethynyl-Fc (further designated as R_4) in **P4** (Scheme 2a). In accordance with these expectations, MALDI-TOF measurements reveal that the quenching with methanol resulted in **P1** having an R_1-starting group and either H- or Br-end groups, whereas the second portion quenched by ZnCl-substituted **4** is almost exclusively represented by a desirable R_1/R_2-functionalized oligomer **P2**, although a small quantity of H- or Br-end functionalizations is

also visible (Fig. 1b). The formation of the Br-terminated product may be attributed to an undesired termination that occurred during the polymerization before the intentional quenching.

According to the MALDI-TOF data, the most abundant polymerization products have DP in the 10–14 range, comparable to the feed ratio of 10 chosen in this experiment. The end group compositions, as well as the DPs of the products, were further deduced by analyzing the ^{1}H-NMR data (Table 1). Particularly, a comparison of integrals of the starting/end groups with the integrals of internal repeat units allowed the determination of DP from ^{1}H-NMR data.[19,47] The thus-obtained DPs are in good agreement with the number average molecular weights (M_n) from SEC measurements (Table 1, Fig. S5†).

The resonance signal of the methyl moiety present in the starting group R_1 appears in the ^{1}H-NMR spectra as a singlet at 2.51 ppm and serves a convenient reference for quantification of the whole spectra. α-Methylene protons of the terminal 3-hexylthiophene repeat unit in the methanol-quenched **P1** appear in the spectra at 2.62 ppm and 2.59 ppm and they correspond to the H- and Br-end functionalized **P1**, respectively (Fig. 2 and S4†). The α-methylene protons of the terminal repeating unit in **P2** (next to the R_2 group) are somewhat shifted to a lower magnetic field (2.69 ppm). Besides the α-methylene protons, protons in aromatic region corresponding to the terminal repeating units (next to the starting and end groups) are also clearly distinguishable in the NMR spectra from the protons of the internal repeating units and they can be employed for the end-group analysis. Particularly, the spectrum of **P2** shows an additional peak at 7.04 ppm that is not observed in **P1** and this peak is assigned to the aromatic proton of the terminal thiophene ring next to the R_2 group. In addition, signals from other terminal thiophenes, such as H/Br-terminated ones in **P1**, could also be resolved at 6.91 ppm for the H-terminated and at 6.84 ppm for the Br-terminated products, which is consistent with the literature data for HT polythiophenes.[48]

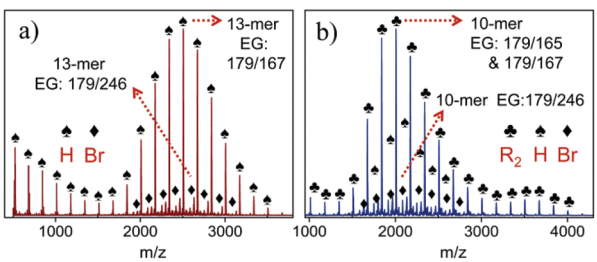

Fig. 1 MALDI-TOF spectra of oligomers **P1** (a) and **P2** (b).

Table 1 M_n, $Đ$, DP and end-group compositions for oligomers **P1**–**P8**

Oligomer/ method	M_n [a] (kg mol^{-1})/DP[b]	$Đ$[a]	Starting-groups: content[b]/kind	End-groups: content[b]/ kind
P1/KCTP	3.4/14	1.11	100/R_1	76/H
P2/KCTP	3.3/12	1.07	100/R_1	53/R_2
P3/KCTP	3.1/10	1.05	100/R_1	70/R_3
P4/KCTP	3.1/10	1.06	100/R_1	74/R_4
P5/GRIM	3.3/12	1.12	58[c]/H	58[c]/H
P6/GRIM	3.1/11	1.18	52[c]/R_2	52[c]/R_2
P7/GRIM	3.3/13	1.09	52[c]/R_3	52[c]/R_3
P8/GRIM	3.1/12	1.09	56[c]/R_4	56[c]/R_4

[a] Determined by SEC in chloroform. [b] Determined by ^{1}H-NMR as described in Fig. S4. [c] Differentiation of the starting-groups from end-groups is difficult for GRIM products, therefore, the provided values refer to an averaged content of the respective groups.

On the other hand, the terminal groups R_1 and R_2 are also easily distinguishable both in the aromatic and aliphatic regions as seen in Fig. 2. Thus, phenyl protons of R_1 in **P2** appear as two doublets (AB system) at 7.58 and 7.44 ppm whereas the corresponding ^{t}Bu group is seen as a singlet at 1.36 ppm in addition to a somewhat up field-shifted singlet (1.35 ppm) of the ^{t}Bu group present in the opposite side (starting group) of the same chain. NOESY ^{1}H–^{1}H NMR experiments were performed for better interpretation of the starting and end group compositions of **P2**.

As seen in Fig. 3, the α-methylene peak of R_2-neighbouring thiophene at 2.69 ppm (g) shows a direct correlation with the doublet peak at 7.44 ppm (h) which belongs to aromatic protons of the R_2 group. Besides, the methyl peak at 2.51 ppm (b) of the starting R_1 group shows correlation with the α-methylene peak of R_1-neighbouring thiophene at 2.77 ppm (d).

Thus, a comparison of integrals corresponding to the reference (methyl-starting group) and all kinds of end groups allows a precise quantification of all the polymerization products regarding their starting- and end-group composition. By applying the above-described end-group analysis, we identified for the methanol-quenched **P1** that all its molecules contain R_1-type starting groups (*i.e.*, 100% starting group functionalization), however two types of end-groups: H (the major fraction, 76%) and Br (24%) from the integral ratio between 2.62 ppm and 2.57 ppm.

The product **P2** is also fully functionalized by desirable starting groups whereas it exhibits a relatively moderate degree of end-group functionalization. As deduced from Fig. 3, only 53% of chains in **P2** contain the desirable R_2-type of end-groups, 38% of H-end groups and 9% of the Br-end groups. In addition, the integral ratio between thiophenic protons corresponding to the R_2-termination (7.04 ppm) (f), H-termination (6.91 ppm) (k) and Br-termination (6.83 ppm) (l) was also used for the quantification of the spectra and these data are in accordance with the results from α-methylene proton analysis.

End group analysis reveals that the product **P3** is fully functionalized by R_1-starting groups and contains 70% of R_3-type end groups and relatively small amounts of undesirable terminations (14% of H and 16% of Br-end groups). Ethynyl-DMA end groups can be quantified by integration of signals from methyl groups in *N*,*N*-dimethylaniline at 3.02 ppm (*N*,*N*-dimethylaniline signals in the aromatic region at 7.41 and 6.69 ppm as well as down-field shifted signals of α-methylene protons next to the R_3-end group, are also observed, Fig. S1†).

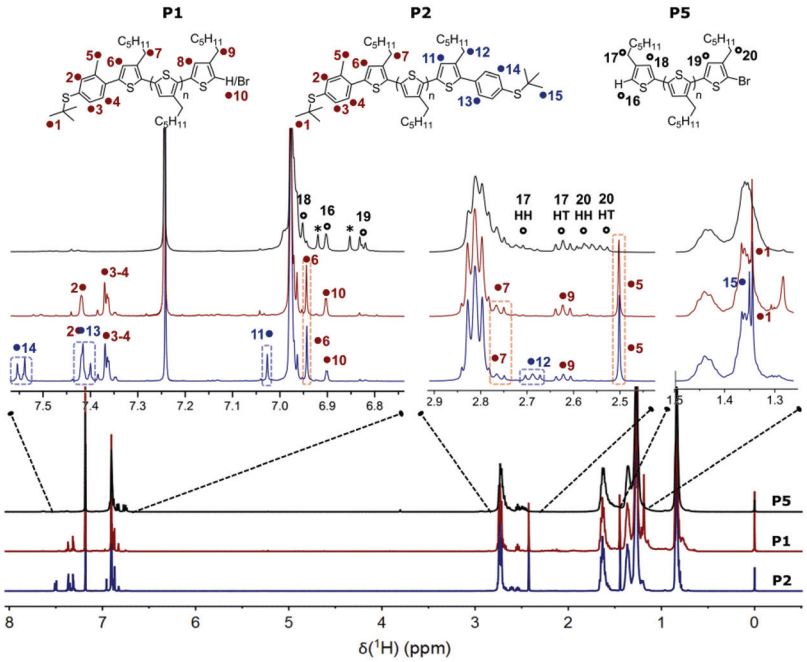

Fig. 2 ^{1}H-NMR spectra of **P1**, **P2** and **P5** (*peaks assignable to the TT coupling).

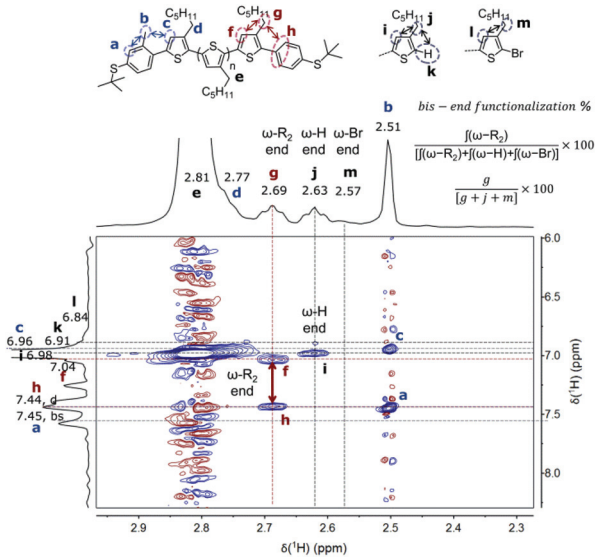

Fig. 3 2D-NOESY ^{1}H–^{1}H NMR spectra of **P2** and end-group assignment; the inset shows the calculation of the bis-end functionalization degree based on integral intensities of the peak at 2.69 ppm, 2.63 ppm, and 2.57 ppm.

Similar to the case of **P3**, the spectrum of ethynyl-Fc terminated product **P4** also has characteristic signals: α-methylene protons at 2.75 ppm, as well as distinct peaks of the ferrocene moiety at 4.53 ppm and 4.28 ppm. By integration of these groups, the content of the ferrocenyl groups R_4 of 74% can be quantified, whereas the content of starting groups approaches 100%.

It is noteworthy that the quantitative starting group functionalization for KCTP-made products **P2–P4** follows not only from a cross-integration of starting- *versus* end-groups but also from the absence of characteristic signals of "reinitiated" products. It is known that one of the major side reactions in KCTP is the disproportionation of initiators leading to the formation of Ni(dppe)Br_2 which initiates the formation of the GRIM-polymerization product having characteristic starting groups of two HH-coupled thiophene rings.[49]

As seen from Fig. 4, which compares the aromatic region of ^{1}H-NMR spectra of the KCTP (**P2**) and the GRIM (**P5**) products, **P2** has no signals at 6.93 ppm and 6.86 ppm assigned to the

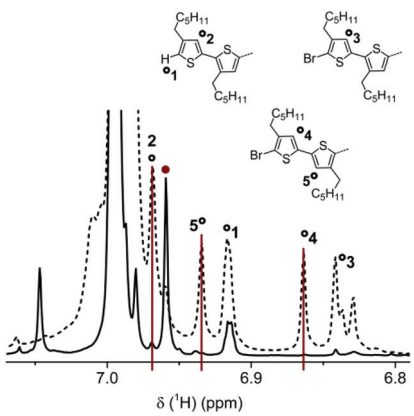

Fig. 4 ^{1}H-NMR spectra of the aromatic region for polymers **P2** (solid line) and **P5** (dashed line) with the specific assignments for HT and TT couplings formed due to the less controlled nature of GRIM polymerization.

reinitiated product. Similarly, the MALDI-TOF data confirm a near quantitative degree of the starting group functionalization (Fig. 5). Considering the peak intensities between R_1-initiated and reinitiated products, high chain initiation efficiencies can be attained by externally prepared R_1-starting group initiated KCTP; oligomer chains were initiated by the R_1-starting group up to 94% for **P1** and 93% for **P2** (see Fig. S2† for chemical structures).

Synthesis of oligo(3-thiophenes) having R_2, R_3 and R_4 end-groups by GRIM polymerization was also performed (Scheme 2b). To this end, polymerization mixtures obtained at the [monomer]/[Ni(dppe)Cl_2] ratio of 10 were quenched with ZnCl-functionalized aryl compounds **4**, **5**, or **6** in a similar manner to that done for KCTP with the difference that twice the amount of the quencher was used in that case. The thus-obtained polymerization products **P5**, **P6**, **P7**, and **P8** were analyzed with regard to their DP, end group content and regioregularity.

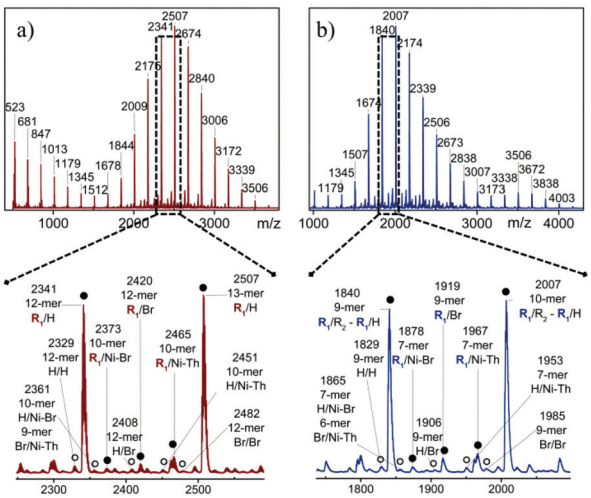

Fig. 5 MALDI-TOF spectra of **P1** (a) and **P2** (b) with enlarged highest molecular weights as inset graphs, showing up to 93% chain initiation by the externally prepared initiator (●); analyzed from MALDI-TOF spectra.

As seen from Table 1, the degrees of R_2/R_2, R_3/R_3 and R_4/R_4 end group functionalizations are equal to 52, 52 and 56%, for GRIM products; **P6**, **P7**, and **P8**, respectively. These values are comparable but somewhat smaller than functionalization degrees achievable with externally initiated KCTP. However, the much higher degree of the starting-group functionalization than the degree of the end-group functionalization, as discussed above for the externally initiated KCTP, demonstrates the much higher fidelity of the chain-initiation than the chain-termination process and shows a clear advantage of KCTP compared to GRIM polymerization. Furthermore, only KCTP provides the synthesis of asymmetrically-functionalized polymers.

Oligomers with strong electron donor moieties, **P3**, **P4**, **P7**, and **P8**, were further converted into their donor–acceptor counterparts **P3-TCBD**, **P4-TCBD**, **P7-TCBD** and **P8-TCBD** by using the Diederich-type reaction with TCNE. This reaction was monitored by ^{1}H-NMR spectroscopy and the quantitative formation of target adducts was observed by down-field shifted resonance signals of DMA and Fc functionalities, both in the aromatic and aliphatic regions.

In order to examine the possible changes in the electronic properties of the oligomers after the introduction of specific end/starting groups, the thus-prepared oligomers were examined by UV-visible absorption and cyclic voltammetry. Several model small molecules were prepared and tested (Fig. 6) for the verification of chemical structures as well as for a better interpretation of optical and electrochemical data. As seen from Fig. 7, the model small molecules **MC-1** and **MC-2** having, besides TCBD, the dimethylaniline and ferrocenyl groups, respectively, exhibit in their absorption spectra characteristic broad charge-transfer bands at 550–750 nm (see also Fig. S9† for the absorption spectra of the corresponding thin films).

Similar bands are also present in oligomers in which TCBD-DMA (**P3**, **P7**) or TCBD-Fc (**P4**, **P8**) were introduced and no such bands are observed in other oligomers (*e.g.*, **P2**). This confirms the successful chemical transformations described above.

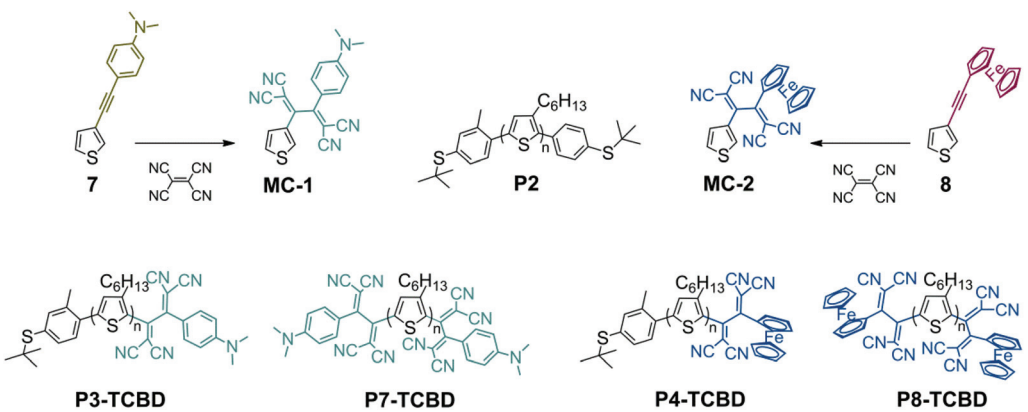

Fig. 6 Chemical structures of oligo(3-hexylthiophene)s and model compounds functionalized with DA chromophores.

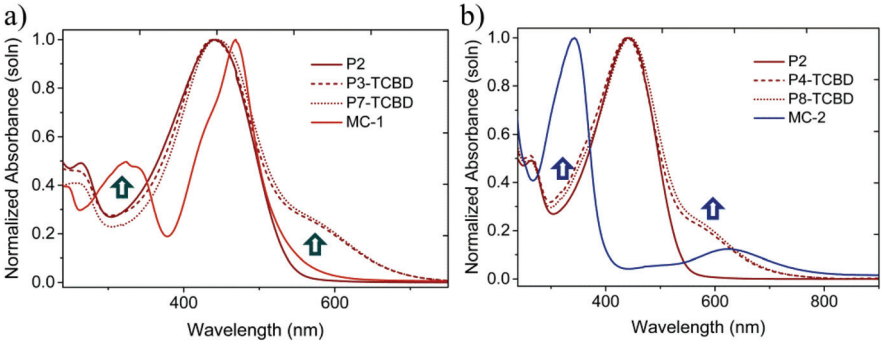

Fig. 7 Normalized absorption spectra in CH_2Cl_2 of TCBD-DMA substituted (a) and TCBD-Fc substituted (b) oligo(3-hexylthiophene)s and the corresponding model compounds.

It is also noteworthy that the GRIM-made oligomers **P7** and **P8** having TCBD-based starting- and end-groups, exhibit only slightly stronger signals in the 550–750 nm region than those observed in KCTP-produced oligomers **P3** and **P4**, having TCBD-based moieties only as the end-groups (for the absorption spectra normalized at the absorption of the oligothiophene backbone). This further confirms the higher efficiency of KCTP as the method for introducing desirable functions. The optical band gaps were also estimated from the absorption onsets and these data are given in Table ESI-2.†

Cyclic voltammetry measurements were performed for the determination of redox activities and HOMO/LUMO energy levels of the obtained materials. The first partly reversible oxidation peak around 0.15 V *versus* the Fc/Fc^+ redox couple may be attributed to the R_1-starting group (sulfide moiety) which is in good agreement with the oxidation profiles of initiator/quencher precursors as seen in Fig. 9. All of the KCTP products containing the R_1 unit as the starting group exhibit the first reversible oxidation peak in the same region (see Fig. 8a), whereas the GRIM products except the ^{t}Bu-terminated product **P6** are deprived of the sharp oxidation peak as observed in Fig. 8b.

As seen from Fig. 8, 10, 11 and Table ESI-2,† cyclic voltammograms of **P2–P8** oligomers and their TCBD adducts displayed several additional reversible oxidation peaks which can be ascribed to morphological non-homogeneity or the co-existence of the zones with different conjugation lengths, which is an expected feature for polythiophene backbones.

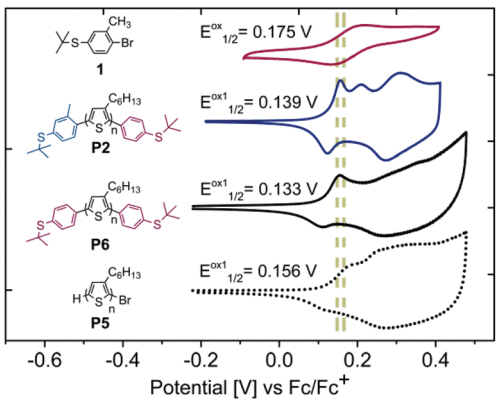

Fig. 9 Oxidation profiles of KCTP product **P2** and GRIM product **P6** containing ^{t}Bu-protected starting/end-groups and the comparison of their oxidation peaks with initiator precursor **1** and un-functionalized GRIM product **P5**.

A partly reversible oxidation peak around 0.2 V *versus* the Fc/Fc^+ redox couple, most likely originates from the oxidation of polymer fragments with the longest conjugation length, whereas the peak around 0.3 V *versus* Fc/Fc^+ may correspond to the amorphous segments with shorter conjugation lengths.[50]

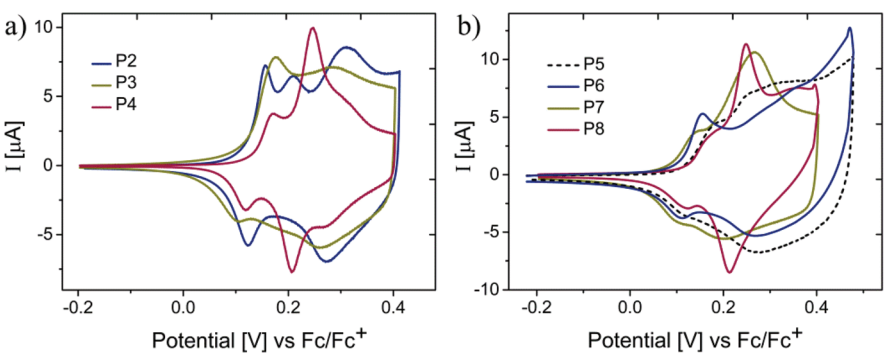

Fig. 8 Comparison of anodic parts of cyclic voltammograms of oligo(3-hexylthiophene)s prepared by KCTP (a); and by GRIM (b).

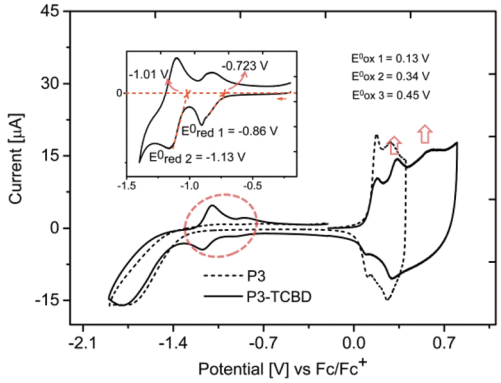

Fig. 10 Cyclic voltammograms for **P3** (dashed line) and **P3-TCBD** (solid line); the inset shows the enlarged cathodic profile of **P3-TCBD**.

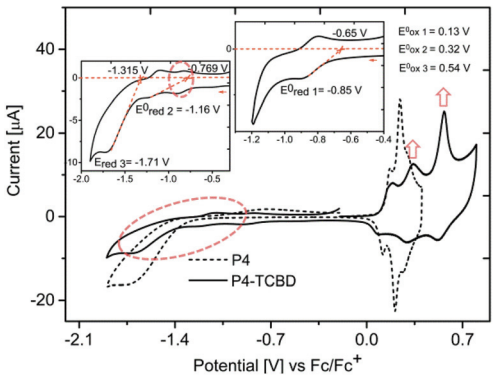

Fig. 11 Cyclic voltammograms of Fc-end group functionalized **P4** (KCTP product) and DA-end group functionalized **P4-TCBD** with well-defined oxidation peaks and maxima potentials; enlarged reduction profiles of **P4-TCBD** with reduction peak maxima and onset potentials (inset graphs).

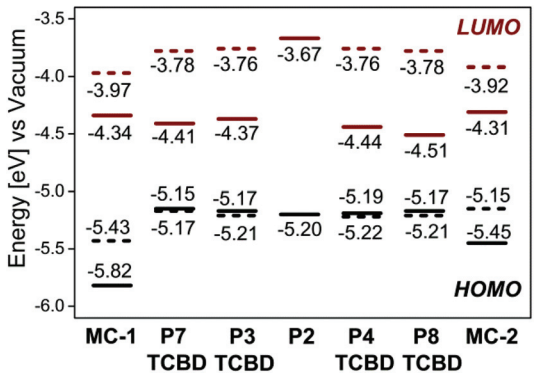

Fig. 12 HOMO–LUMO energy levels for the donor-substituted (dashed lines) and respective DA-substituted (solid lines) oligomers and model compounds.

Hence, the number of consecutive redox peaks and shifts in peak potentials upon oxidation strongly depend on the content of HT–HT couplings on the polymer sequence for unfunctionalized polyalkylthiophenes.[50] Yet, in this study, these changes in oxidation profiles cannot be attributed solely to the distortion of planarity by the addition of TT couplings along the rr-O3HT backbone. The shape of the oxidation peaks varies strongly for differently-terminated oligomers. This can be attributed to a different termination pattern and a different content of redox-active (and electron-rich/deficient) units in the oligomers. GRIM oligomers are expected to show more indistinctive and slightly anodically shifted oxidation peaks than their KCTP counterparts due to a loss in the HT coupling content and an increase in the donor-functionalized end-group content, as seen in Fig. 8. Thus, the oxidative pattern of the oligomers can be finely tuned by changing not only the end-group functionality but also the degree of their regioregularity.

The introduction of the TCBD moiety into the oligomers mostly changes the reduction part of the voltammograms. The appearance of two quasi-reversible reduction waves at −0.86 V and −1.13 V for **P3-TCBD** and at −0.87 V and −1.15 V for **P7-TCBD** can be attributed to the presence of redox active TCBD, as observed in model compound **MC-1** in similar but much stronger redox processes (see Fig. S10 and S12a†).

In contrast, for TCBD-Fc functionalized oligomers, the oxidation peaks were not simply distinguishable due to the inhibition from intense ferrocene peaks. Similarly, for TCBD-Fc functionalized oligomers, the end group DA functionality can be deduced from the cathodically shifted reduction peak like −0.86 V for **P4-TBCD**, −0.84 V for **P8-TCBD** and −0.93 V for **MC-2** (Fig. 11). **P4-TCBD** and **P8-TCBD**, conversely, showed only two slightly seen reversible reduction peaks; the former at −0.86 V and −0.84 V, corresponding to the first distinct reduction of **MC-2** (see Fig. S11 and S12b†).

Since oxidation happens with the removal of electrons from the HOMO, delocalized along the π-conjugated backbone mostly coming from thiophene units, and reduction with the addition of electrons to the LUMO, onset potentials from first oxidation/reduction peaks are expected to be closely related to the HOMO–LUMO energy levels.

Fig. 12 represents the CV-determined HOMO–LUMO energy levels for the oligomers before (dashed lines) and after the functionalization with TCNE (solid lines). The data clearly indicated that the LUMO levels for all oligomers decreased dramatically upon the formation of the TCBD moiety and the extent of LUMO lowering was more significant when compared to the changes in the HOMO levels. Accordingly, the electrochemical band gaps were reasonably decreased after each click post-functionalization and in good agreement with optical band gaps (see Table ESI-2†).

Conclusions

Herein, we employed quasi-living externally-initiated nickel-catalyzed KCTP to obtain well-defined end-functionalized oligo(3-hexylthiophene) conductive wires having a controlled molecular weight and quantitative degree of the starting-group

functionality. Termination of the KCTP process with different ZnCl-functionalized species provided a satisfactory (60–70%) degree of the end-group functionality.

These data demonstrate the much higher fidelity of the chain-initiation than that of the chain-termination process which highlights a clear advantage of KCTP compared to the GRIM polymerization for the synthesis of bis-functionalized conductive wires; furthermore, KCTP is the only method for the preparation of asymmetrically-functionalized polythiophenes. The introduction of functional groups into oligomers *via* the Diederich-type click reaction allows fine adjustment of their electronic (HOMO/LUMO) levels. The functionalized molecular wires having starting and end-groups of different kinds open up new opportunities for applications in molecular electronics. In this case, one can benefit not only from a selective binding of the molecular wire to electrodes made of different metals (to achieve site-specific positioning of the wires) but also from different charge-injection properties of the end- *versus* starting-groups providing a rectification effect. These issues will be studied in future works.

Experimental

All reactions were carried out under an argon atmosphere unless otherwise mentioned. All reagents and solvents were used without further purification. 2.0 M i-PrMgCl solution in THF, 2.5 M ^{n}BuLi solution in hexane, $ZnCl_2$, and all catalysts ($Ni(dppe)Cl_2$, $Pd(PPh_3)_2Cl_2$, $Pd(PPh_3)_4$) were stored and used in a glove box. i-PrMgCl and ^{n}BuLi were purchased as solutions and used without further dilution. Precursor compounds for polymerizations were synthesized by several different reactions; the precursors for model compounds **MC-1** and **MC-2** by a Sonogashira cross-coupling reaction and all synthetic details can be found in the ESI.† All polymerization reactions, post-polymerization modifications and all other experimental and characterization details are also given in the ESI.† Size exclusion chromatography (SEC) measurements were performed using chloroform as eluent at the flow rate of 1 mL min^{-1} for 1 mg ml^{-1} polymer solutions on an Agilent 1260 Infinity Series (Agilent, USA), equipped with a refractive index detector and a Resipore/PLgel 5 μm Mixed-C main column. All samples were filtered through 0.20 μm PTFE syringe filters before measurements. The number average molecular weights (M_n), weight average molecular weights (M_w) and dispersity indexes ($Đ$-DI) were determined by calibration with polystyrene standards. Nuclear Magnetic Resonance (NMR) measurements were conducted for ^{1}H and ^{13}C nuclei. ^{1}H (500.1 MHz) and ^{13}C (125.8 MHz) NMR spectra were recorded on a Bruker Biospin Avance III spectrometer using a 5 mm probe. Chemical shifts were reported in ppm downfield from $SiMe_4$ and internally referenced with the solvent's residual signal, $CDCl_3$; δ (^{1}H) = 7.27 ppm, δ (^{13}C) = 77.0 ppm. In addition to ^{1}H and ^{13}C 1D-NMR experiments, precise chemical structures of polymers were determined by the appearance/absence of correlation and neighboring peaks from the NOESY (^{1}H–^{1}H) spectra. Matrix-assisted laser desorption ionization time-of-flight (MALDI-TOF) spectra were recorded on an Autoflex Speed TOF/TOF System (Bruker Daltonics GmbH). The measurements were carried out in reflector mode and positive polarity by using a pulsed smart beam laser (modified Nd:YAG laser). The ion acceleration voltage was set to 20 kV. For the sample preparation, the polymers were mixed with *trans*-2-(3-(4-*tert*-butylphenyl)-2-methyl-2-propenylidene) malononitrile (DCTB) as the sample matrix and both were dissolved in THF. The preparation was done with the addition of sodium trifluoroacetate (NaTFAc) as a cationized salt. Absorption spectra were recorded with a Specord 40 (Analytikjena) UV/visible spectrometer; solution absorbance measurements were carried out in 1 cm quartz cuvettes with dry CH_2Cl_2 while thin film absorbances were measured from the films prepared by dropcasting from CH_2Cl_2 solutions of materials on glass substrates. Cyclic voltammetry experiments were performed with an Ivium-n-Stat potentiostat in a three electrode single-compartment cell with a platinum (Pt) disc working electrode, a platinum wire counter electrode and an $Ag/Ag^{+}/CH_3CN_{(dry)}/(0.1\ M)\ Bu_4NPF_6$ reference electrode under a nitrogen atmosphere, at a speed of 50 mV s^{-1}. The films of the oligo(3-hexylthiophene) wires were deposited onto the Pt working electrode by drop-casting from dichloromethane solution (2 mg ml^{-1}). All oxidation & reduction potentials were referenced against the half-wave potential of the ferrocene/ferrocenium (Fc/Fc^{+}) redox couple. The HOMO–LUMO levels were calculated by setting Fc/Fc^{+}_{vac} at −5.1 eV *vs.* vacuum and onset potentials were determined from the first reversible oxidation/reduction waves.[51]

Acknowledgements

This work was supported by the Initiative and Networking Fund of the Helmholtz Association of German Research Centers through the International Helmholtz Research School for Nanoelectronic Networks, IHRS NANONET (VH-KO-606) and the Graduate Academy of TU Dresden. The authors are also grateful for support from DFG (grant KI-1094/9). We also thank Dr Hartmut Komber for recording and discussion of NMR spectra.

Notes and references

1 C. Joachim, J. K. Gimzewski and A. Aviram, *Nature*, 2000, **408**, 541.
2 J. C. Cuevas and E. Scheer, *Molecular Electronics: An Introduction to Theory and Experiment*, World Scientific Publishing Co. Pte Ltd, Singapore, 2010; M. Kiguchi and S. Kaneko, *Phys. Chem. Chem. Phys.*, 2013, **15**, 2253.
3 R. Yamada, H. Kumazawa, S. Tanaka and H. Tada, *Appl. Phys. Express*, 2009, **2**, 025002.
4 J. S. Schumm, D. L. Pearson, L. Jones, R. Hara and J. M. Tour, *Nanotechnology*, 1996, **7**, 430; L. Venkataraman, J. E. Klare, C. Nuckolls, M. S. Hybertsen and

M. L. Steigerwald, *Nature*, 2006, **442**, 904; W. Hong, H. Li, S.-X. Liu, Y. Fu, J. Li, V. Kaliginedi, S. Decurtins and T. Wandlowski, *J. Am. Chem. Soc.*, 2012, **134**, 19425; P. Moreno-Garcia, M. Gulcur, D. Z. Manrique, T. Pope, W. Hong, V. Kaliginedi, C. Huang, A. S. Batsanov, M. R. Bryce, C. J. Lambert and T. Wandlowski, *J. Am. Chem. Soc.*, 2013, **135**, 12228; C. R. Arroyo, S. Tarkuc, R. Frisenda, J. S. Seldenthuis, C. H. M. Woerde, R. Eelkema, F. C. Grozema and H. S. J. van der Zant, *Angew. Chem., Int. Ed.*, 2013, **52**, 3152.

5 H. Gronbeck, A. Curioni and W. Andreoni, *J. Am. Chem. Soc.*, 2000, **122**, 3839; J. G. Kushmerick, D. B. Holt, S. K. Pollack, M. A. Ratner, J. C. Yang, T. L. Schull, J. Naciri, M. H. Moore and R. Shashidhar, *J. Am. Chem. Soc.*, 2002, **124**, 10654; D. Vonlanthen, A. Mishchenko, M. Elbig, M. Neuburger, T. Wandlowski and M. Mayor, *Angew. Chem., Int. Ed.*, 2009, **48**, 8886; C. M. Guedon, H. Valkenier, T. Markussen, K. S. Thygesen, J. C. Hummelen and S. J. van der Molen, *Nat. Nanotechnol.*, 2012, **7**, 305; E. H. van Dijk, D. J. T. Myles, M. H. van der Veen and J. C. Hummelen, *Org. Lett.*, 2006, **8**, 2333.

6 T. J. J. Müller, *Functional Organic Materials*, Wiley, 2007.

7 W. Hong, D. Z. Manrique, P. Moreno-Garcia, M. Gulcur, A. Mishchenko, C. J. Lambert, M. R. Bryce and T. Wandlowski, *J. Am. Chem. Soc.*, 2012, **134**, 2292.

8 W. P. Hu, J. Jiang, H. Nakashima, Y. Luo, Y. Kashimura, K. Q. Chen, Z. Shuai, K. Furukawa, W. Lu, Y. Q. Liu, D. B. Zhu and K. Torimitsu, *Phys. Rev. Lett.*, 2006, **96**, 027801.

9 J. J. W. M. Rosink, M. A. Blauw, L. J. Geerligs, E. van der Drift, B. A. C. Rousseeuw, S. Radelaar, W. G. Sloof and E. J. M. Fakkeldij, *Langmuir*, 2000, **16**, 4547.

10 T. L. Choi, K. H. Lee, W. J. Joo, S. Lee, T. W. Lee and M. Y. Chae, *J. Am. Chem. Soc.*, 2007, **129**, 9842.

11 Q. Lu, K. Liu, H. M. Zhang, Z. B. Du, X. Wang and F. S. Wang, *ACS Nano*, 2009, **3**, 3861; S. Kubatkin, A. Danilov, M. Hjort, J. Cornil, J. L. Bredas, N. Stuhr-Hansen, P. Hedegard and T. Bjornholm, *Nature*, 2003, **425**, 698; S. H. Choi, C. Risko, M. C. Ruiz Delgado, B. Kim, J. L. Bredas and C. D. Frisbie, *J. Am. Chem. Soc.*, 2010, **132**, 4358; D. L. Pearson and J. M. Tour, *J. Org. Chem.*, 1997, **62**, 1376.

12 C. D. Varnado and C. W. Bielawski, *Polymer Science: A Comprehensive Reference*, 2012, vol. 5, p. 175.

13 S. H. Choi, B. Kim and C. D. Frisbie, *Science*, 2008, **320**, 1482; S. H. Choi and C. D. Frisbie, *J. Am. Chem. Soc.*, 2010, **132**, 16191; X. Zhao, C. Huang, M. Gulcur, A. S. Batsanov, M. Baghernejad, W. Hong, M. R. Bryce and T. Wandlowski, *Chem. Mater.*, 2013, **25**, 4340; G. J. Ashwell, B. Urasinska, C. Wang, M. R. Bryce, I. Gracec and C. J. Lambert, *Chem. Commun.*, 2006, 4706; R. Sondergaard and F. C. Krebs, *Polymers*, 2011, **3**, 545; N. Tuccitto, V. Ferri, M. Cavazzini, S. Quici, G. Zhavnerko, A. Licciardello and M. A. Rampi, *Nat. Mater.*, 2009, **8**, 41; S. Taniguchi, M. Minamoto, M. M. Matsushita, T. Sugawara, Y. Kawada and D. Bethell, *J. Mater. Chem.*, 2006, **16**, 3459; M. Endou, Y. Ie, T. Kaneda and Y. Aso, *J. Org. Chem.*, 2007, **72**, 2659; Y. Ie, M. Endou, S. K. Lee, R. Yamada, H. Tada and Y. Aso, *Angew. Chem., Int. Ed.*, 2011, **50**, 11980; R. G. Hicks and M. B. Nodwell, *J. Am. Chem. Soc.*, 2000, **122**, 6746; D. Bong, I. Tam and R. Breslow, *J. Am. Chem. Soc.*, 2004, **126**, 11796; R. Yamada, H. Kumazawa, S. Tanaka and H. Tada, *Appl. Phys. Express*, 2009, **2**, 025002; R. Yamada, H. Kumazawa, T. Noutoshi, S. Tanaka and H. Tada, *Nano Lett.*, 2008, **8**, 1237.

14 L. Luo, S. H. Choi and C. D. Frisbie, *Chem. Mater.*, 2011, **23**, 631.

15 J. L. Bredas, G. B. Street, B. Themans and J. M. Andre, *J. Chem. Phys.*, 1985, **83**, 1323; J. L. Bredas and A. J. Heeger, *Macromolecules*, 1990, **23**, 1150.

16 L. Zhang, N. S. Colella, F. Liu, S. Trahan, J. K. Baral, H. H. Winter, S. C. B. Mannsfeld and A. L. Briseno, *J. Am. Chem. Soc.*, 2013, **135**, 844; A. Mishra, C.-Q. Ma and P. Bauerle, *Chem. Rev.*, 2009, **109**, 1141; T. Izumi, S. Kobashi, K. Takimiya, Y. Aso and T. Otsubo, *J. Am. Chem. Soc.*, 2003, **125**, 5286; N. Sumi, H. Nakanishi, S. Ueno, K. Takimiya, Y. Aso and T. Otsubo, *Bull. Chem. Soc. Jpn.*, 2001, **74**, 979; T. Otsubo, Y. Aso and K. Takimiya, *Bull. Chem. Soc. Jpn.*, 2001, **74**, 1789.

17 F. P. V. Koch, P. Smith and M. Heeney, *J. Am. Chem. Soc.*, 2013, **135**, 13695.

18 Y. Ie, M. Endou, A. Han, R. Yamada, H. Tada and Y. Aso, *Pure Appl. Chem.*, 2012, **84**, 931.

19 A. Kiriy, V. Senkovskyy and M. Sommer, *Macromol. Rapid Commun.*, 2011, **32**, 1503.

20 Y. H. Geng, L. Huang, S. P. Wu and F. S. Wang, *Sci. China: Chem.*, 2010, **53**, 1620.

21 T. Yokozawa and A. Yokoyama, *Chem. Rev.*, 2009, **109**, 5595.

22 R. Tkachov, V. Senkovskyy, M. Horecha, U. Oertel, M. Stamm and A. Kiriy, *Chem. Commun.*, 2010, **46**, 1425.

23 R. Tkachov, V. Senkovskyy, T. Beryozkina, K. Boyko, V. Bakulev, A. Lederer, K. Sahre, B. Voit and A. Kiriy, *Angew. Chem., Int. Ed.*, 2014, **53**, 2402.

24 I. Osaka and R. D. McCullough, *Acc. Chem. Res.*, 2008, **41**, 1202.

25 E. L. Lanni and A. J. McNeil, *J. Am. Chem. Soc.*, 2009, **131**, 16573–16579; K. Okamoto and C. K. Luscombe, *Polym. Chem.*, 2011, **2**, 2424.

26 N. Marshall, S. K. Sontag and J. Locklin, *Chem. Commun.*, 2011, **47**, 5681.

27 A. Yokoyama, R. Miyakoshi and T. Yokozawa, *Macromolecules*, 2004, **37**, 1169.

28 H. A. Bronstein and C. K. Luscombe, *J. Am. Chem. Soc.*, 2009, **131**, 12894.

29 V. Senkovskyy, N. Khanduyeva, H. Komber, U. Oertel, M. Stamm, D. Kuckling and A. Kiriy, *J. Am. Chem. Soc.*, 2007, **129**, 6626.

30 V. Senkovskyy, R. Tkachov, T. Beryozkina, H. Komber, U. Oertel, M. Horecha, V. Bocharova, M. Stamm, S. A. Gevorgyan, F. C. Krebs and A. Kiriy, *J. Am. Chem. Soc.*, 2009, **131**, 16445.

31 V. Senkovskyy, M. Sommer, H. Komber, R. Tkachov, W. Huck and A. Kiriy, *Macromolecules*, 2010, **43**, 10157.

32 R. S. Loewe, S. M. Khersonsky and R. D. McCullough, *Adv. Mater.*, 1999, **11**, 250.
33 K. Okamoto and C. K. Luscombe, *Chem. Commun.*, 2014, **50**, 5310.
34 A. Smeets, P. Willot, J. De Winter, P. Gerbaux, T. Verbiest and G. Koeckelberghs, *Macromolecules*, 2011, **44**, 6017.
35 N. Doubina, S. A. Paniagua, A. V. Soldatova, A. K. Y. Jen, S. R. Marder and C. K. Luscombe, *Macromolecules*, 2011, **44**, 512.
36 F. Monnaie, W. Brullot, T. Verbiest, J. De Winter, P. Gerbaux, A. Smeets and G. Koeckelberghs, *Macromolecules*, 2013, **46**, 8500.
37 S. L. Fronk, C.-K. Mai, M. Ford, R. P. Noland and G. C. Bazan, *Macromolecules*, 2015, **48**, 6224.
38 The oligothiophenes are very important bridges in D–B–A systems, for example, see: T.-G. Zhang, Y. Zhao, I. Asselberghs, A. Persoons, K. Clays and M. J. Therien, *J. Am. Chem. Soc.*, 2005, **127**, 9710.
39 S. Kato and F. Diederich, *Chem. Commun.*, 2010, **46**, 1994.
40 This transformation was firstly reported by Bruce *et al.*: M. I. Bruce, J. R. Rodgers, M. R. Snow and A. G. Swincer, *J. Chem. Soc., Chem. Commun.*, 1981, 271.
41 Y. Yuan and T. Michinobu, *J. Polym. Sci., Part A: Polym. Chem.*, 2011, **49**, 225.
42 T. Michinobu, H. Kumazawa, K. Noguchi and K. Shigehara, *Macromolecules*, 2009, **42**, 5903.
43 T. Shoji, S. Ito, K. Toyota, M. Yasunami and N. Morita, *Chem. – Eur. J.*, 2008, **14**, 8398.
44 T. Michinobu, *Chem. Soc. Rev.*, 2011, **40**, 2306.
45 A. Blaszczyk, M. Elbing and M. Mayor, *Org. Biomol. Chem.*, 2004, **2**, 2722.
46 M. Mayor, H. B. Weber, J. Reichert, M. Elbing, C. von Hanisch, D. Beckmann and M. Fischer, *Angew. Chem., Int. Ed.*, 2003, **42**, 5834.
47 F. Monnaie, L. Verheyen, J. D. Winter, P. Gerbaux, W. Brullot, T. Verbiest and G. Koechelberghs, *Macromolecules*, 2015, **48**(24), 8752.
48 G. Barbarella, A. Bongini and M. Zambianchi, *Macromolecules*, 1994, **27**, 3039.
49 One should also take into account that this HH defect can "move" from the chain starting toward the middle of the chain owing to the "ring-walking" process: R. Tkachov, V. Senkovskyy, H. Komber, J.-U. Sommer and A. Kiriy, *J. Am. Chem. Soc.*, 2010, **132**(22), 7803.
50 M. Skompska and A. Szkurlat, *Electrochim. Acta*, 2001, **46**, 4007.
51 C. M. Cardona, W. Li, A. E. Kaifer, D. Stockdale and G. C. Bazan, *Adv. Mater.*, 2011, **23**, 2367.